

Mixed-Ligand Lanthanide Complexes Supported by Ditopic Bis(Imino-methyl)-Phenol/Calix[4]arene Macrocycles: Synthesis, Structures, and Luminescence Properties of $[Ln_2(L^2)(MeOH)_2]$ ($Ln = La, Eu, Tb, Yb$)

Steve Ullmann,^{a,b} Peter Hahn,^a Parvathy Mini,^c Kellie L. Tuck,^c Axel Kahnt,^d Bernd Abel,^{d,e} Matias E. G. Suburu,^{f,g} Cristian A. Strassert,^{f,g} and Berthold Kersting^{a*}

^a Institut für Anorganische Chemie, Universität Leipzig, Johannisallee 29, 04103 Leipzig, Germany, E-mail: b.kersting@uni-leipzig.de Fax: +49(0)341-97-36199

^b Institut für Nichtklassische Chemie e.V., Permoserstraße 15, D-04318 Leipzig, Germany

^c School of Chemistry, Monash University, Clayton, Victoria 3800, Australia

^d Leibniz Institute of Surface Engineering (IOM), Department of Functional Surfaces, Permoserstr. 15, D-04318 Leipzig, Germany

^e Wilhelm-Ostwald-Institut für Physikalische und Theoretische Chemie, Universität Leipzig, Linnéstraße 2, D-04103 Leipzig, Germany

^f Institut für Anorganische und Analytische Chemie, CiMIC, SoN - Westfälische Wilhelms-Universität Münster - Corrensstraße 28/30, 48149 Münster, Germany

^g CeNTech - Westfälische Wilhelms-Universität Münster - Heisenbergstraße 11, 48149 Münster, Germany

Supporting Information

Content

1. Analytical data for $[La_2(L^2)(MeOH)_2]$ (**1**)
2. Analytical data for $[Eu_2(L^2)(MeOH)_2]$ (**2**)
3. Analytical data for $[Tb_2(L^2)(MeOH)_2]$ (**3**)
4. Analytical data for $[Yb_2(L^2)(MeOH)_2]$ (**4**)
5. Spectrophotometric titrations / Determination of Stability Constants
6. Determination of Coordination Geometries
7. Luminescence Properties of $[HNEt_3][Eu_2(HL_1)(L_1)]$, $[HNEt_3][Tb_2(HL_1)(L_1)]$, $[Eu_2(L^2)(MeOH)_2]$ (**2**) and $[Tb_2(L^2)(MeOH)_2]$ (**3**)

1. Analytical data for $[\text{La}_2(\text{L}^2)(\text{MeOH})_2]$ (1)

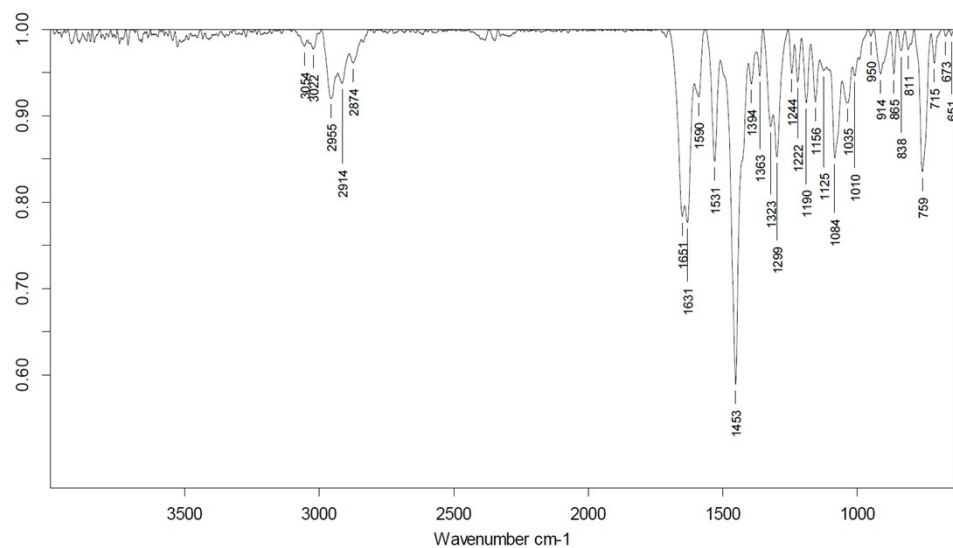


Fig S1. FT-IR spectrum of **1**.

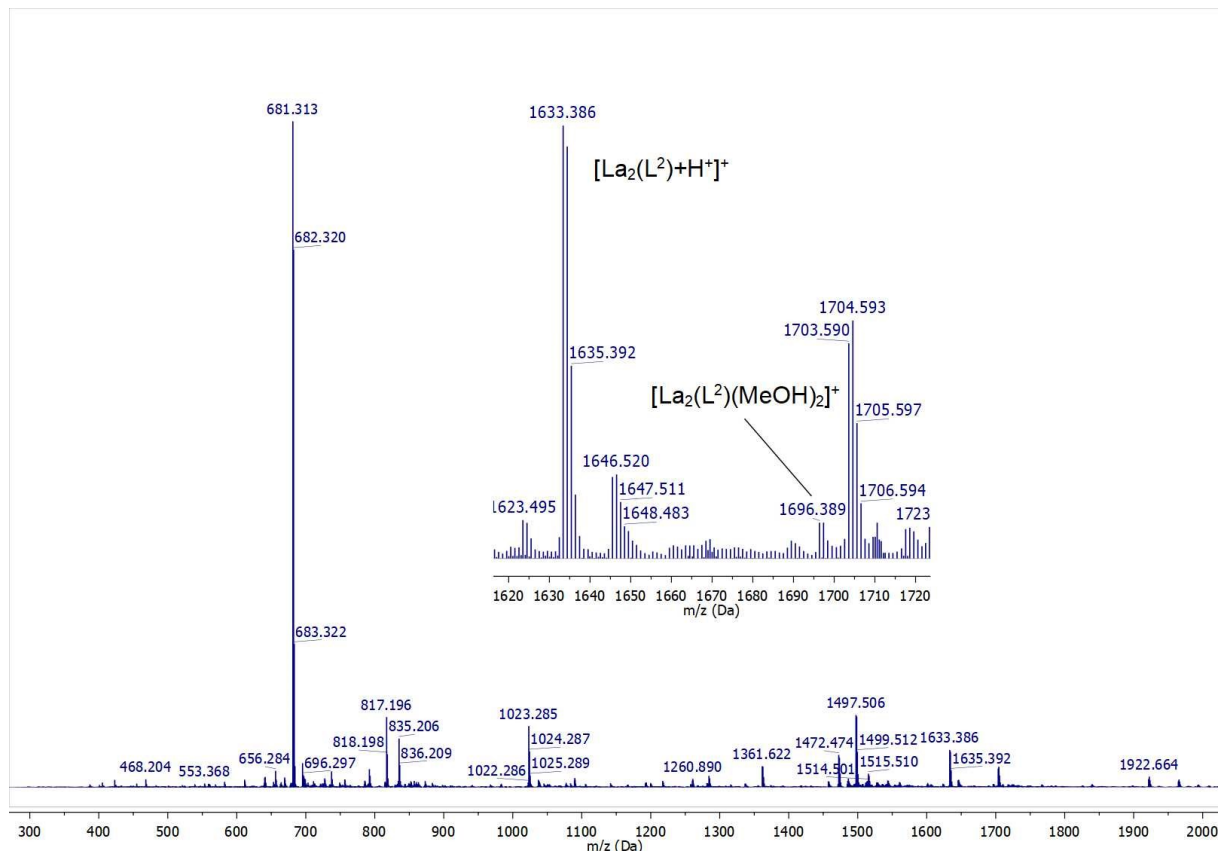


Fig. S2. ESI mass spectrum of **1** (MeOH/CH₂Cl₂ solution, 10⁻⁵ M). The ESI mass spectrum showed peaks for the dinuclear La^{III} complex, but with very low intensity, suggesting a rather labile nature under the experimental conditions. The signal at $m/z = 1633.386$ (inset) and $m/z = 1696.389$ can be attributed to $[\text{La}_2(\text{L}^2)+\text{H}^+]$ ⁺ and $[\text{La}_2(\text{L}^2)(\text{MeOH})_2]$ ⁺ cations.

Analytical data for $[\text{Eu}_2(\text{L}^2)(\text{MeOH})_2]$ (2)

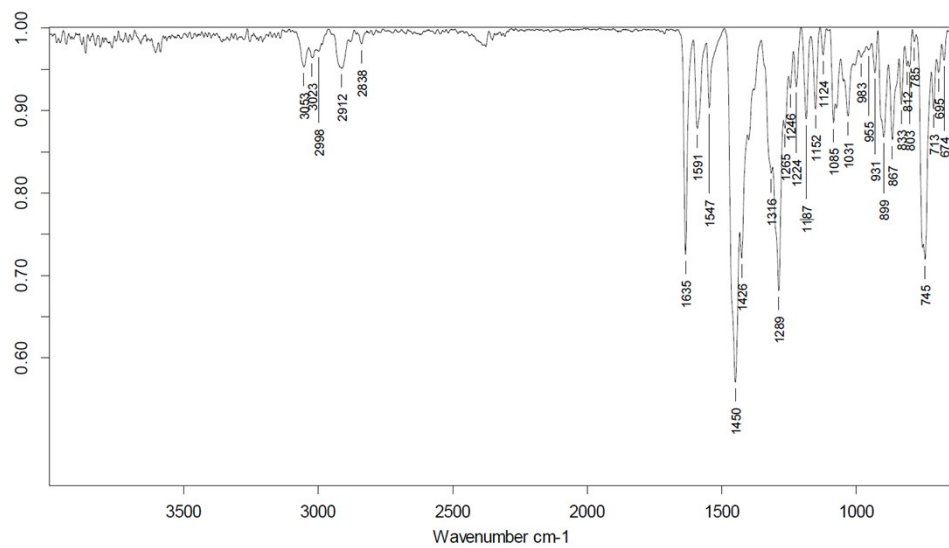


Fig. S3. FT-IR spectrum of 2.

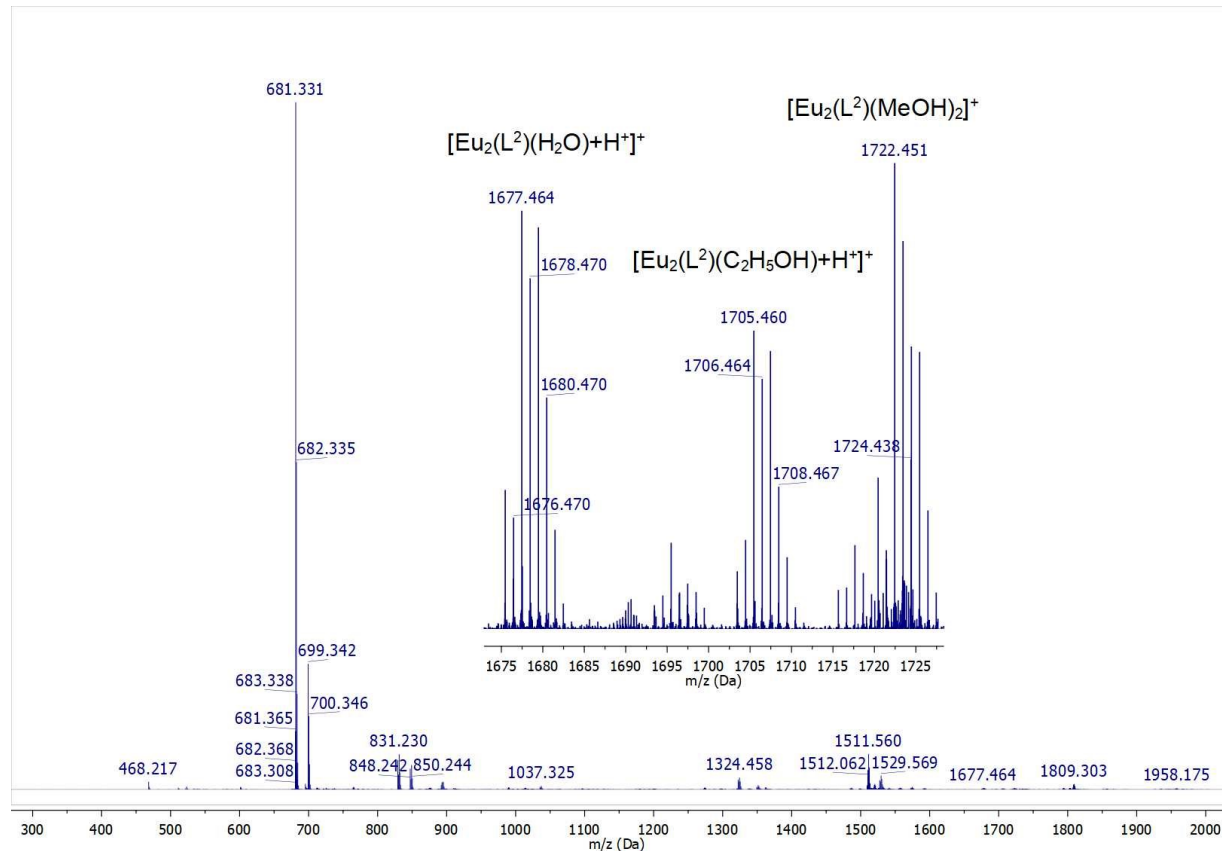


Fig. S4. ESI mass spectrum of 2 (mixed MeOH/EtOH/CH₂Cl₂ solution, 10⁻⁵ M). The ESI mass spectrum showed peaks for the dinuclear Eu^{III} complex but with very low intensity. The signals at *m/z* 1677.464 (inset) and at 1722.451 can be attributed to $[\text{Eu}_2(\text{L}^2)(\text{H}_2\text{O})+\text{H}^+]^+$ and $[\text{Eu}_2(\text{L}^2)(\text{MeOH})_2]^+$ cations, respectively.

2. Analytical data for $[\text{Tb}_2(\text{L}^2)(\text{MeOH})_2]$ (3)

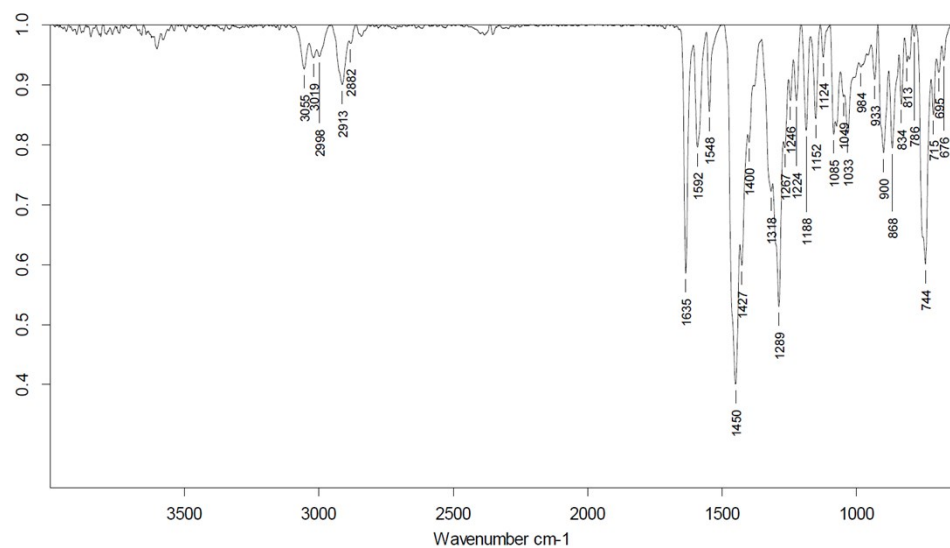


Fig. S5. FT-IR spectrum of **3**.

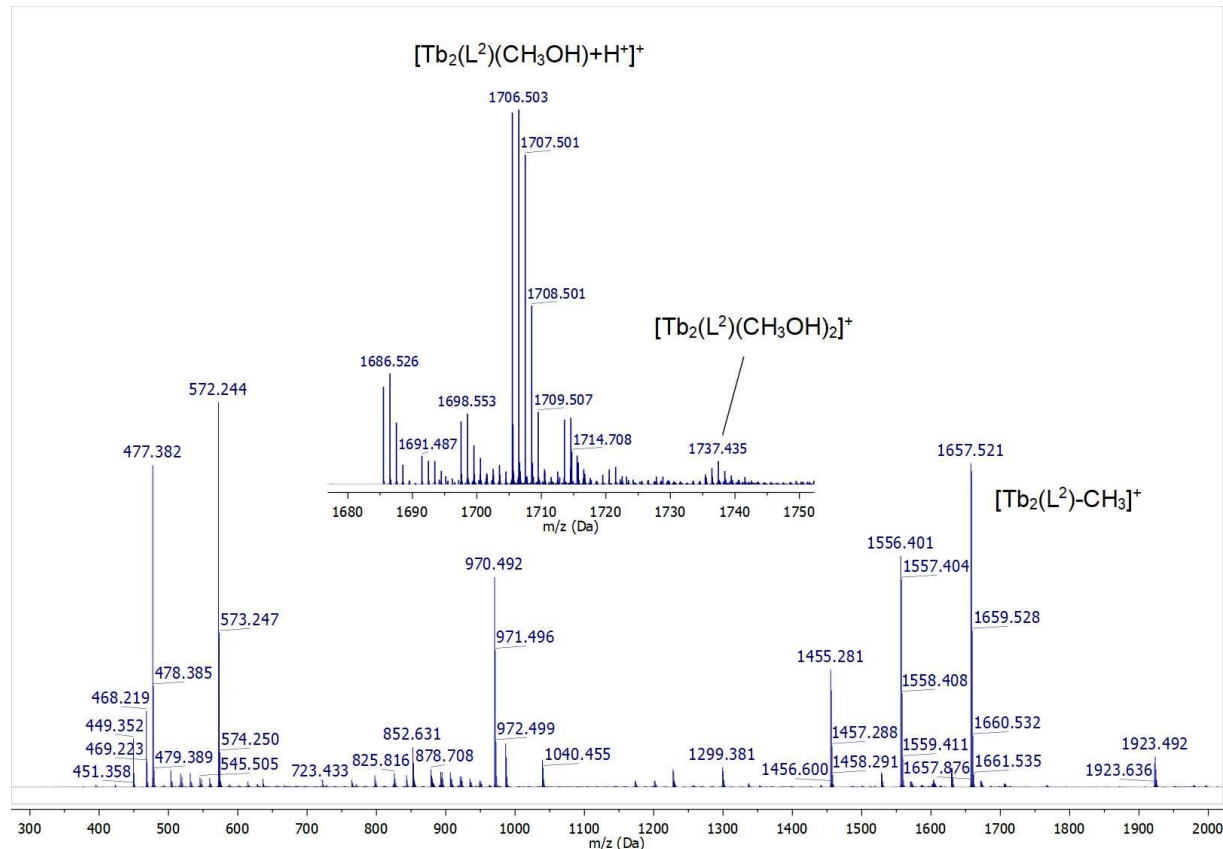


Fig. S6. ESI mass spectrum of **3** (mixed MeOH/CH₂Cl₂ solution, 10⁻⁵ M). The ESI-MS spectrum showed only weak signals at *m/z* 1705.500 and 1737.435 attributable to dinuclear [Tb₂(L²)(MeOH)+H]⁺ and [Tb₂(L²)(MeOH)₂]⁺ cations, respectively. The base peak at 681.313 seen in the spectra of **1**, **2** and **4** is absent in this case for yet unknown reasons.

3. Analytical data for $[Yb_2(L^2)]$ (4)

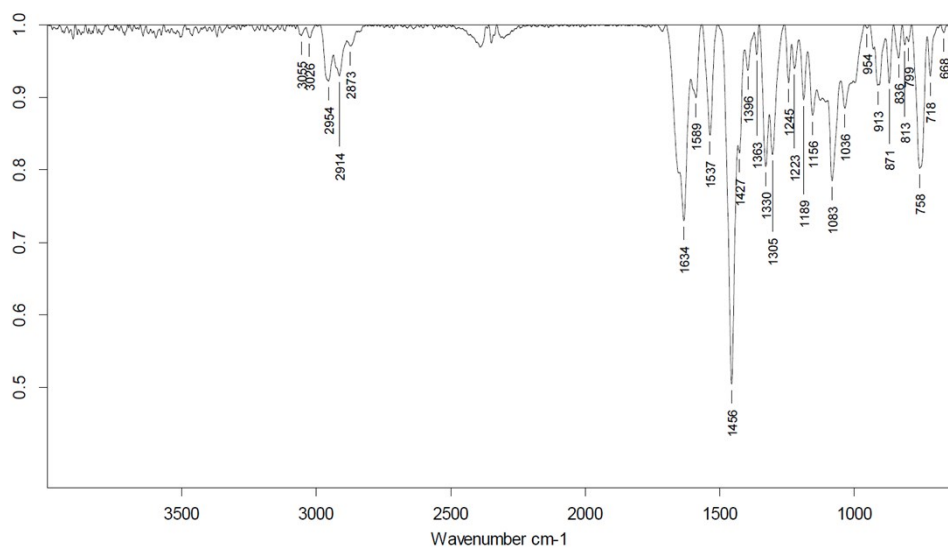


Fig S7. FT-IR spectrum of 4.

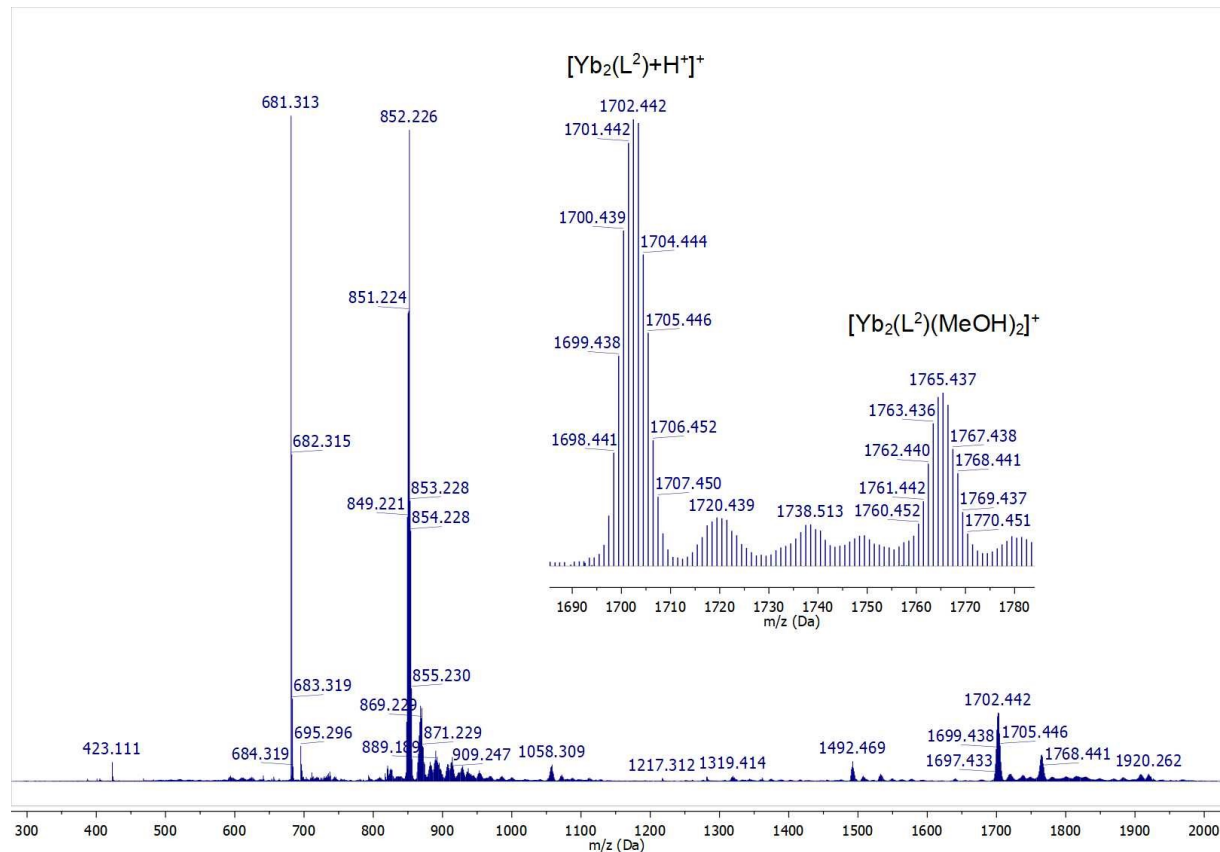


Fig. S8. ESI mass spectrum of 4 (mixed MeOH/CH₂Cl₂ solution, 10⁻⁵ M). The ESI-MS spectrum showed only a weak signal at m/z 1765.437 which corresponds to a $[Yb_2(L^2)(MeOH)_2]^+$ cation.

4. Spectrophotometric titrations / Determination of Stability Constants

Batch data for $[\text{La}_2(\text{L}^2)(\text{MeOH})_2]$ (1)

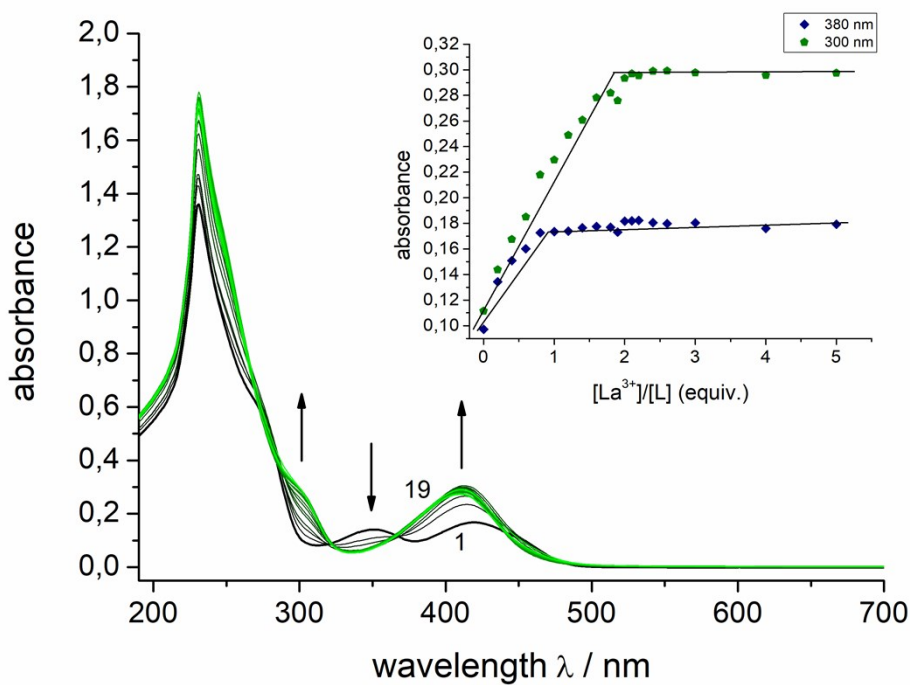


Fig. S9. Spectrophotometric titration of H_6L^2 with $\text{La}(\text{NO}_3)_3 \cdot 6\text{H}_2\text{O}$ in a $\text{CH}_2\text{Cl}_2/\text{MeOH}$ (1/1 v/v) solvent mixture ($2 \cdot 10^{-5}$ M concentration) at constant ionic strength (10^{-2} M $\text{N}^n\text{Bu}_4\text{PF}_6$, $T = 298$ K) in the presence of $2 \cdot 10^{-4}$ M NEt_3 . The green curve refers to a final molar ratio of $\text{M}/\text{H}_6\text{L}^2 = 5.0$. The inset shows the evolution of selected absorbance values versus the $[\text{La}^{3+}]/[(\text{L}^2)^{6-}]$ molar ratio.

HypeSpec refinement output (see main text for titration conditions)

Project title: Titration of H_6L^2 by $\text{La}(\text{NO}_3)_3$
Converged in 1 iterations with sigma = 3.4384

		standard
Log beta	value	deviation
$[\text{La}(\text{L}^2)]$	5.4163	0.0485
$[\text{La}_2(\text{L}^2)]$	11.4865	0.0549

Correlation coefficients

2 0.442

1

Parameter numbers

1 $[\text{La}(\text{L}^2)]$

2 $[\text{La}_2(\text{L}^2)]$

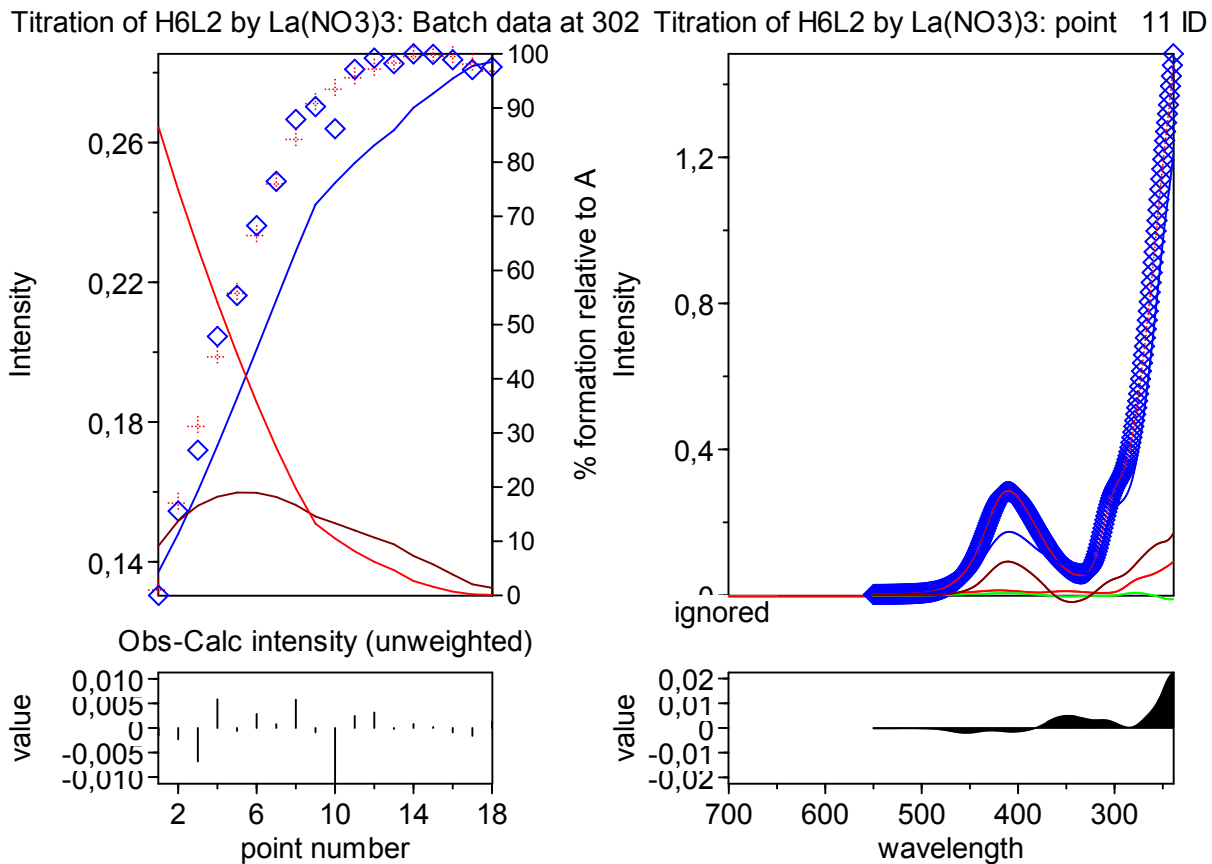


Fig. S10. Titration isotherm extracted at 302 nm (left panel), spectrum corresponding to the 11th data point (right panel), and plot of residuals (bottom panels). Observed absorbance values are plotted as blue diamonds and the calculated ones as red crosses. The solid lines in the right panel show the calculated contribution of H₆L² (red), La(No₃)₃ (green), the 1:1 complex (brown) and the 1:2 complex (blue) to the total absorbance.

Batch data for [Eu₂(L²)(MeOH)₂] (2)

HypeSpec refinement output (see main text for titration conditions)

Project title: Titration of H₆L² by Eu(No₃)³
Converged in 1 iterations with sigma = 4.0091

		standard
Log beta	value	deviation
[Eu(L ²)]	6.0139	0.0686
[Eu ₂ (L ²)]	12.0494	0.0911

Correlation coefficients
2 0.741
1

Parameter numbers
1 [Eu(L²)]
2 [Eu₂(L²)]

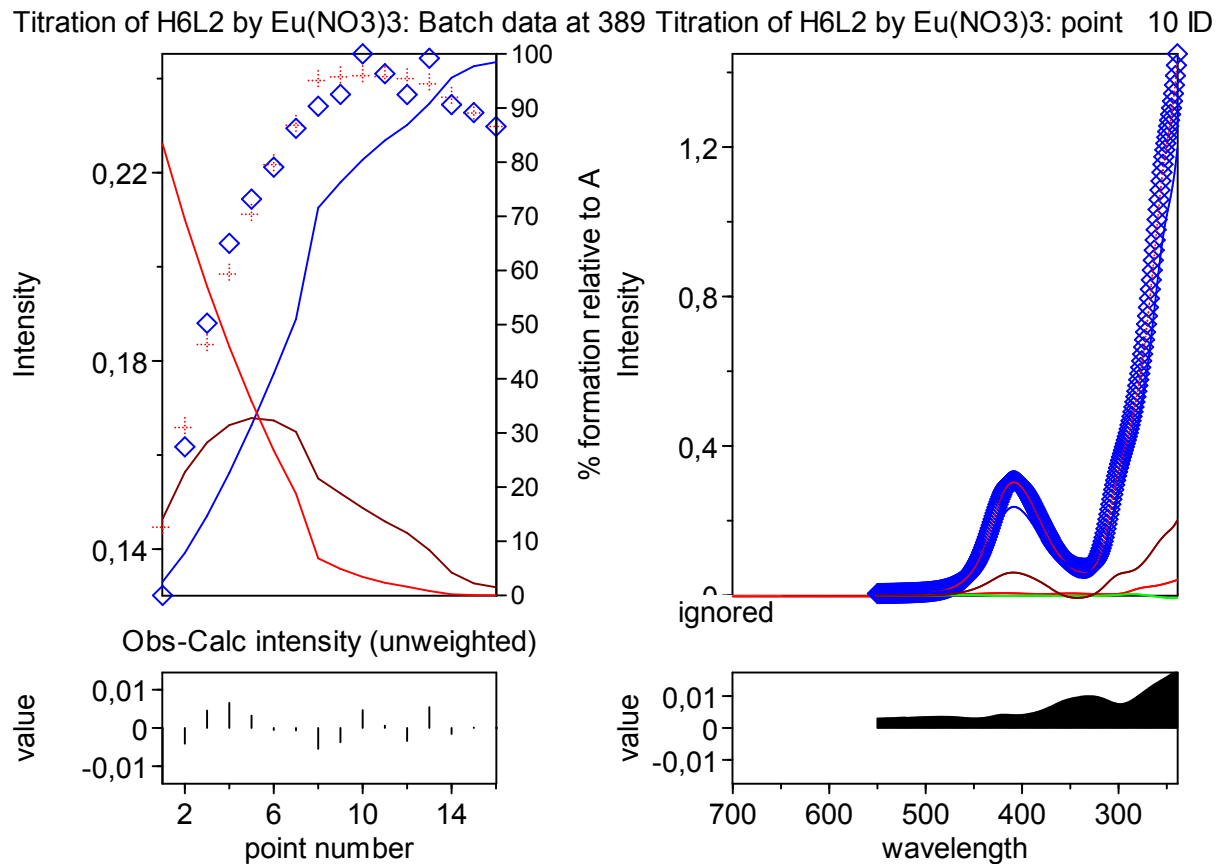


Fig. S11. Titration isotherm extracted at 389 nm (left panel), spectrum corresponding to the 10th data point (right panel), and plot of residuals (bottom panels). Observed absorbance values are plotted as blue diamonds and the calculated ones as red crosses. The solid lines in the right panel show the calculated contribution of H₆L²⁻ (red), Eu(NO₃)₃ (green), the 1:1 complex (brown) and the 1:2 complex (blue) to the total absorbance.

Batch data for $[\text{Tb}_2(\text{L}^2)(\text{MeOH})_2]$ (3)

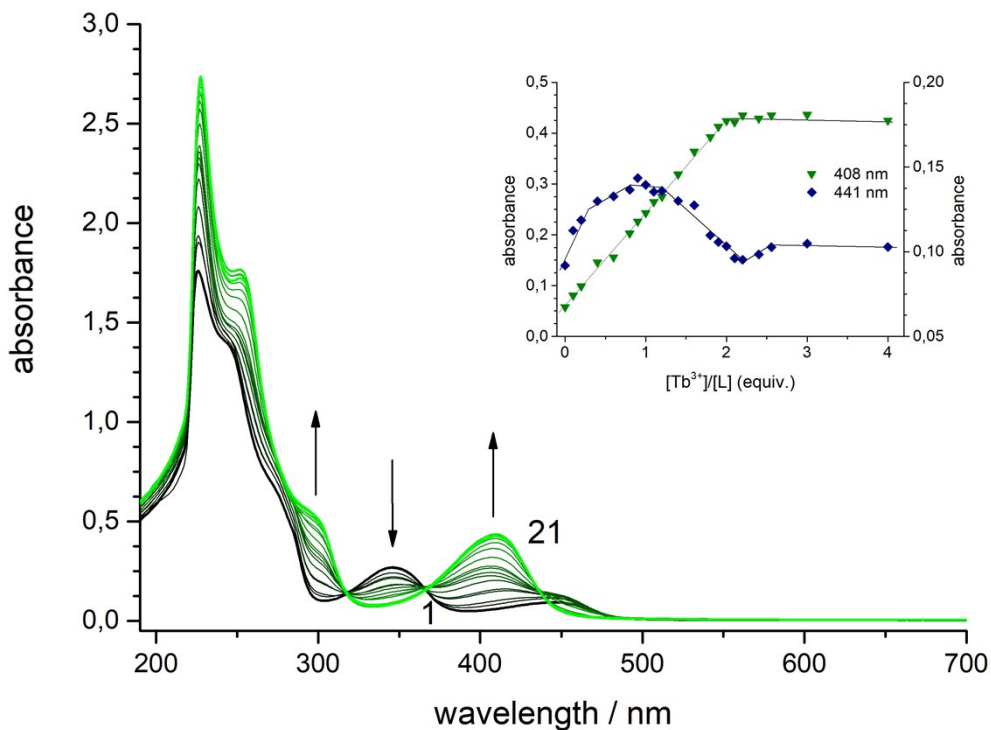


Fig. S12. Spectrophotometric titration of H_6L^2 with $\text{Tb}(\text{NO}_3)_3 \cdot 6\text{H}_2\text{O}$ in a $\text{CH}_2\text{Cl}_2/\text{MeOH}$ (1/1 v/v) solvent mixture ($2.5 \cdot 10^{-5}$ M concentration) at constant ionic strength (10^{-2} M $\text{N}^n\text{Bu}_4\text{PF}_6$, $T = 298$ K) in the presence of $2 \cdot 10^{-4}$ M NEt_3 . The green curve refers to a final molar ratio of $\text{M}/\text{H}_6\text{L}^2 = 4.0$. The inset shows the evolution of selected absorbance values versus the $[\text{Tb}^{3+}]/[(\text{L}^2)^{6-}]$ molar ratio.

HypeSpec refinement output (see main text for titration conditions)

Project title: Titration of H_6L^2 by $\text{Tb}(\text{NO}_3)_3$
Converged in 1 iterations with sigma = 2.6220

		standard
Log beta	value	deviation
$[\text{Tb}(\text{L}^2)]$	6.5596	0.0605
$[\text{Tb}_2(\text{L}^2)]$	13.2028	0.1025

Correlation coefficients

2 0.918

1

Parameter numbers

1 $[\text{Tb}(\text{L}^2)]$

2 $[\text{Tb}_2(\text{L}^2)]$

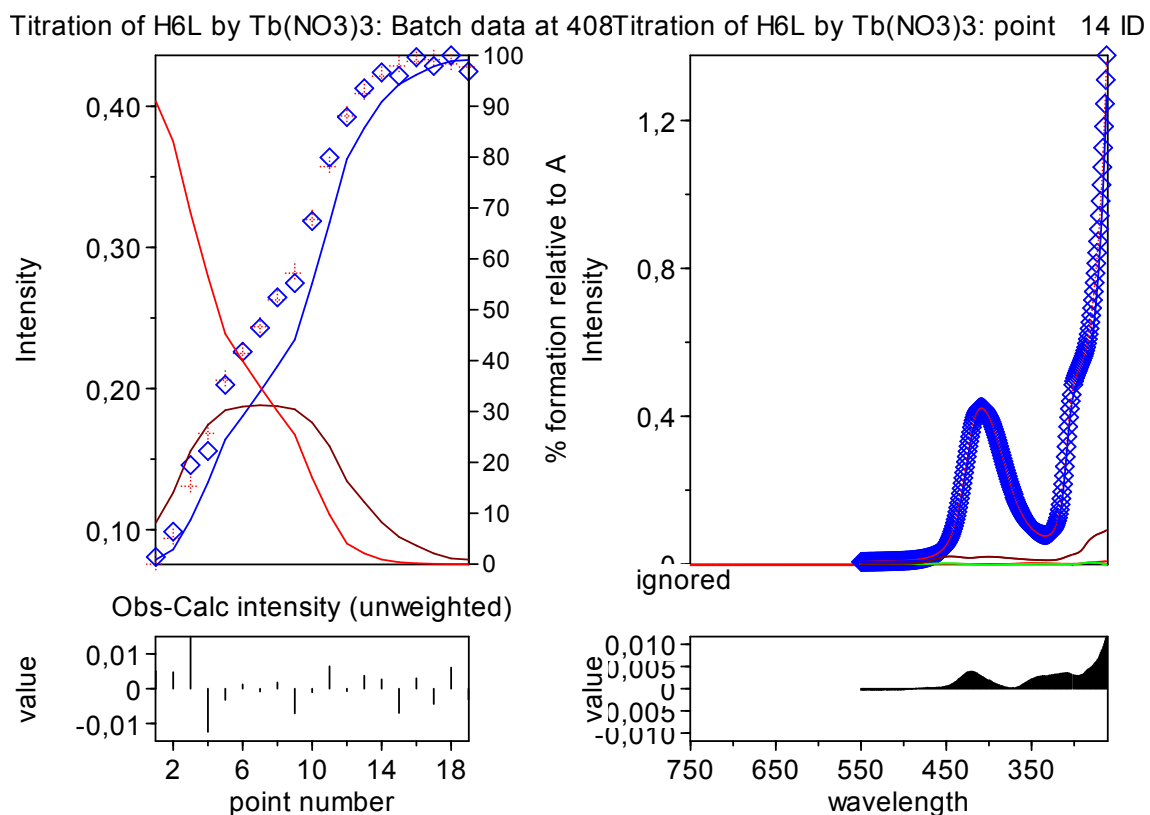


Fig. S13. Titration isotherm extracted at 408 nm (left panel), spectrum corresponding to the 14th data point (right panel), and plot of residuals (bottom panels). Observed absorbance values are plotted as blue diamonds and the calculated ones as red crosses. The solid lines in the right panel show the calculated contribution of H₆L² (red), Tb(No₃)₃ (green), the 1:1 complex (brown) and the 1:2 complex (blue) to the total absorbance.

Batch data for $[Yb_2(L^2)(MeOH)_2]$ (4)

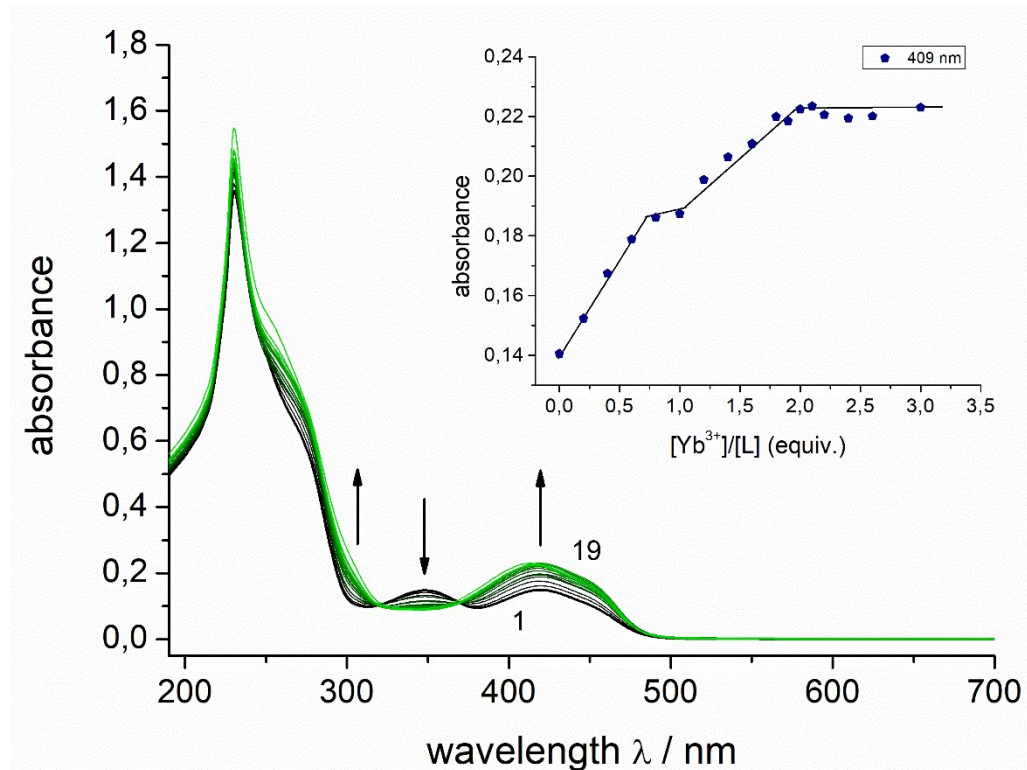


Fig. S14. Spectrophotometric titration of H_6L^2 with $Yb(NO_3)_3 \cdot 5H_2O$ in a $CH_2Cl_2/MeOH$ (1/1 v/v) solvent mixture ($2 \cdot 10^{-5}$ M concentration) at constant ionic strength (10^{-2} M $N^nBu_4PF_6$, $T = 298$ K) in the presence of $2 \cdot 10^{-4}$ M NEt_3 . The green curve refers to a final molar ratio of $M^{3+}/H_6L^2 = 5.0$. The inset shows the evolution of selected absorbance values versus the $[Yb^{3+}]/[(L^2)^{6-}]$ molar ratio.

HypeSpec refinement output (see main text for titration conditions)

Project title: Titration of H_6L^2 by $Yb(NO_3)_3$
 Converged in 1 iterations with sigma = 1.0518

		standard
Log beta	value	deviation
$[Yb(L^2)]$	5.2480	0.0772
$[Yb_2(L^2)]$	11.5752	0.0766

Correlation coefficients

2 0.468

1

Parameter numbers

1 $[Yb(L^2)]$

2 $[Yb_2(L^2)]$

Titration of H₆L₂ by Yb(No₃)₃: Batch data at 409 nm Titration of H₆L₂ by Yb(No₃)₃: point 12 ID

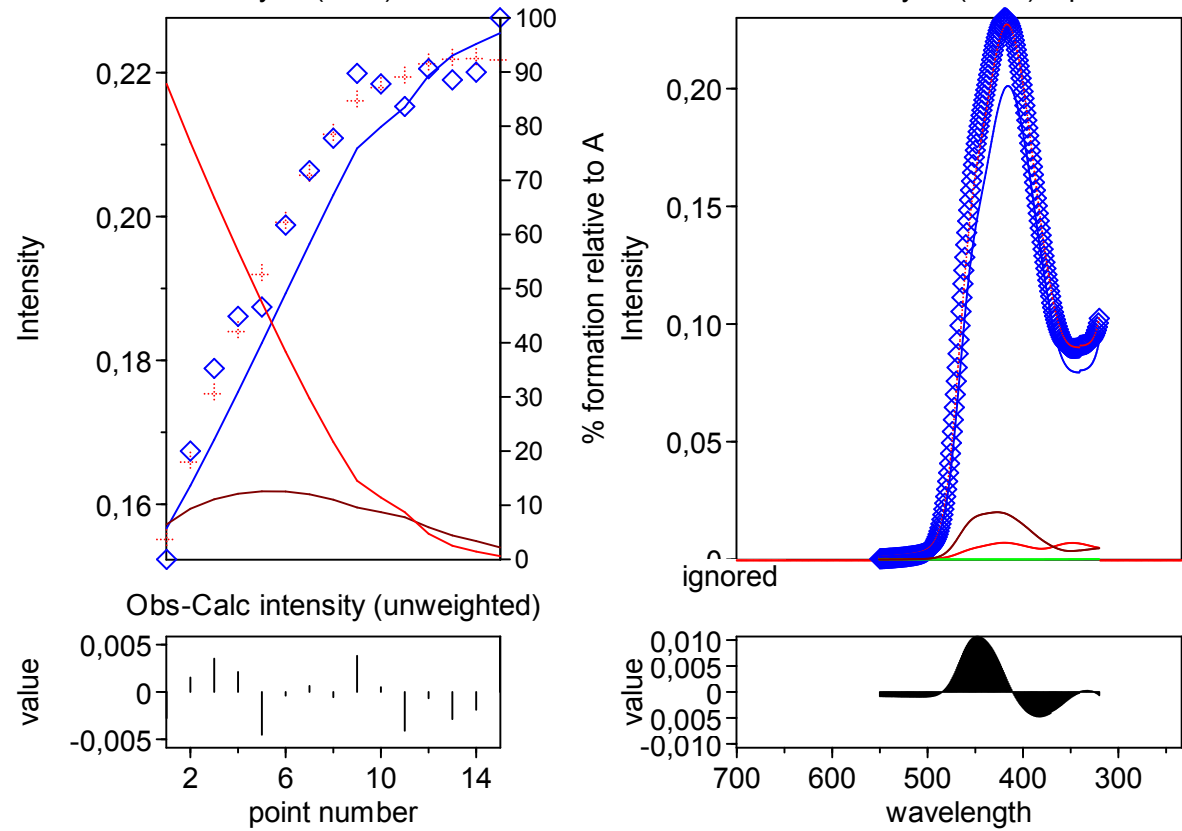


Fig. S15. Titration isotherm extracted at 409 nm (left panel), spectrum corresponding to the 12th data point (right panel), and plot of residuals (bottom panels). Observed absorbance values are plotted as blue diamonds and the calculated ones as red crosses. The solid lines in the right panel show the calculated contribution of H₆L₂ (red), Yb(No₃)₃ (green), the 1:1 complex (brown) and the 1:2 complex (blue) to the total absorbance.

6. Determination of Coordination Geometries

Determination of Coordination Geometries utilizing SHAPE

The coordination geometries of the lanthanide ion in complexes $[\text{HNEt}_3][\text{Ln}_2(\text{HL}^1)(\text{L1})]$ and $[\text{Ln}_2(\text{L}^2)_2(\text{MeOH})_2]$ were examined utilizing the SHAPE program.¹ According to SHAPE, deviations from ideal coordination geometry are represented by a symmetry factor, that increases upon increasing distortions from the ideal geometry, for which the deviation factor is zero.

Several coordination environments were considered for the seven-coordinate Eu^{3+} ions in $(\text{HNEt}_3)[\text{Eu}_2(\text{HL}^1)(\text{L1})]$. According to SHAPE, the coordination geometry is best described as intermediate between a **capped octahedron** and a **capped trigonal prismatic coordination geometry**.

Compound ^{a)}			$(\text{HNEt}_3)[\text{Ln}_2(\text{HL}^1)(\text{L1})]$	
Coordination Geometry	Abbreviation	Symmetry	Symmetry Factor Ln1	Symmetry Factor Ln2
Heptagon	HP-7	D_{7h}	29.097	30.205
Hexagonal pyramid	HPY-7	C_{6v}	17.958	19.332
Pentagonal bipyramidal	PBPY-7	D_{5h}	4.519	4.050
Capped octahedron	COC-7	C_{3v}	2.257	2.368
Capped trigonal prism	CTPR-7	C_{2v}	2.616	2.369
Johnson pentagonal bipyramidal J13	JPBPY-7	D_{5h}	7.260	6.941
Johnson elongated triangular pyramid J7	JETPY-7	C_{3v}	16.624	16.584

a) Data refer to the crystal structure of the Gd complex.

According to SHAPE, the coordination geometry of the seven-coordinate Ln^{3+} ions in the $[\text{Ln}_2(\text{L}^2)(\text{MeOH})_2]$ complexes is best described as a **capped octahedral (for Eu1)** or **capped trigonal octahedral (Eu2, Tb1, Tb2)**. The other complexes ($\text{Ln} = \text{La}, \text{Yb}$) are assumed to be isostructural to the Eu and Tb complexes and to exhibit similar coordination environments.

Compound			$[\text{Eu}_2(\text{L}^2)(\text{MeOH})_2]$	$[\text{Tb}_2(\text{L}^2)(\text{MeOH})_2]$		
Coordination Geometry	Abbreviation	Symmetry	Factor Eu1	Factor Eu2	Factor Tb1	Factor Tb2
Heptagon	HP-7	D_{7h}	30.309	30.048	29.446	30.526
Hexagonal pyramid	HPY-7	C_{6v}	18.806	20.891	20.301	20.734
Pentagonal bipyramidal	PBPY-7	D_{5h}	6.605	4.932	6.540	5.620
Capped octahedron	COC-7	C_{3v}	1.428	1.821	1.760	1.493
Capped trigonal prism	CTPR-7	C_{2v}	1.917	1.300	1.125	1.309
Johnson pentagonal bipyramidal J13	JPBPY-7	D_{5h}	8.558	7.666	8.522	8.385
Johnson elongated triangular pyramid J7	JETPY-7	C_{3v}	15.979	18.148	17.086	16.506

7. Luminescence Properties of $[\text{HNEt}_3][\text{Eu}_2(\text{HL}^1)(\text{L}^1)]$, $[\text{HNEt}_3][\text{Tb}_2(\text{HL}^1)(\text{L}^1)]$, $[\text{Eu}_2(\text{L}^2)(\text{MeOH})_2]$ (**2**) and $[\text{Tb}_2(\text{L}^2)(\text{MeOH})_2]$ (**3**)

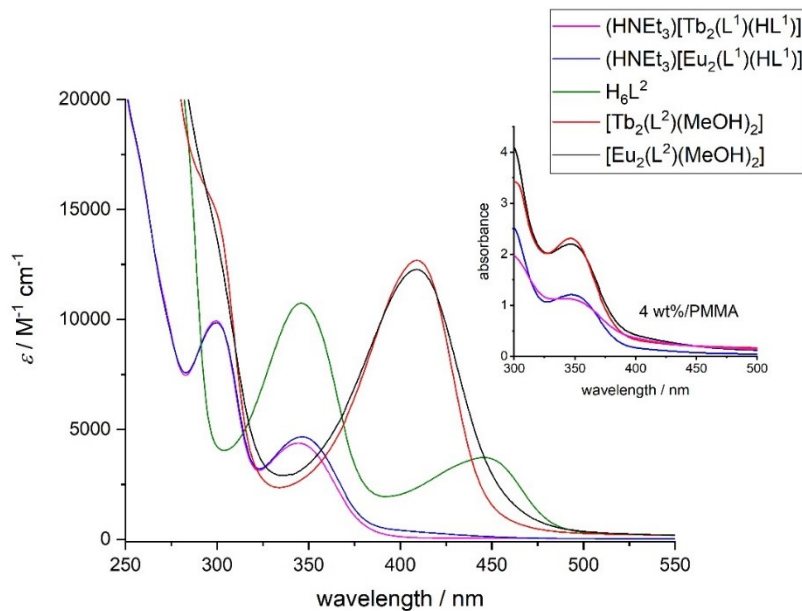


Fig. S16. UV–vis absorption spectra of H_6L^2 , $[\text{Eu}_2(\text{L}^2)(\text{MeOH})_2]$ (**2**), $[\text{Tb}_2(\text{L}^2)(\text{MeOH})_2]$ (**3**) ($2.5 \cdot 10^{-5}$ M concentration), $[\text{HNEt}_3][\text{Eu}_2(\text{HL}^1)(\text{L}^1)]$ and $[\text{HNEt}_3][\text{Tb}_2(\text{HL}^1)(\text{L}^1)]$ ($5 \cdot 10^{-5}$ M) in $\text{CH}_2\text{Cl}_2/\text{MeOH}$ (1/1, v/v) at 298 K. Inset: spectra of PMMA films 4 wt% doped with the respective complexes (thickness ≈ 0.2 mm).

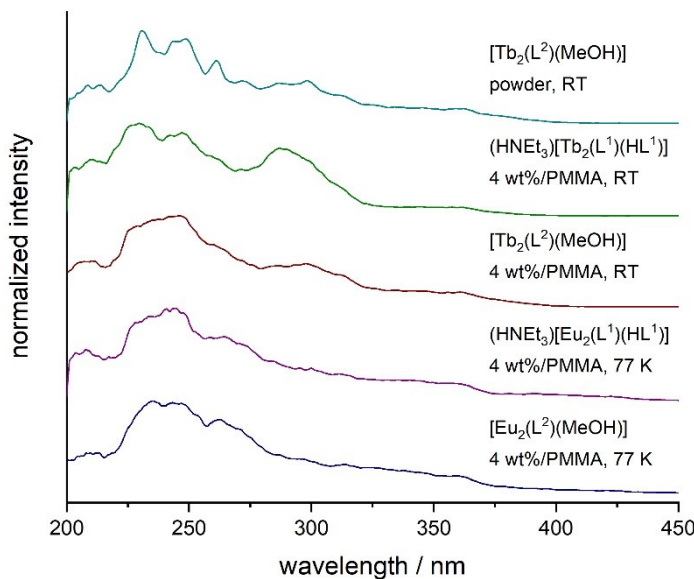


Fig. S17. Excitation spectra of $[\text{HNEt}_3][\text{Eu}_2(\text{HL}^1)(\text{L}^1)]$, $[\text{HNEt}_3][\text{Tb}_2(\text{HL}^1)(\text{L}^1)]$, $[\text{Eu}_2(\text{L}^2)(\text{MeOH})_2]$ (**2**), and $[\text{Tb}_2(\text{L}^2)(\text{MeOH})_2]$ (**3**) at 77 K and 298 K immobilized in a PMMA thin film (4 wt%, thickness ~ 0.2 mm) and in the solid state for **3** upon monitoring at 615 nm (Eu^{3+}) and 545 nm (Tb^{3+}).

6. Photoluminescence properties of $[\text{Eu}_2(\text{L}^2)(\text{MeOH})_2]$ (**2**) and $[\text{Tb}_2(\text{L}^2)(\text{MeOH})_2]$ (**3**)

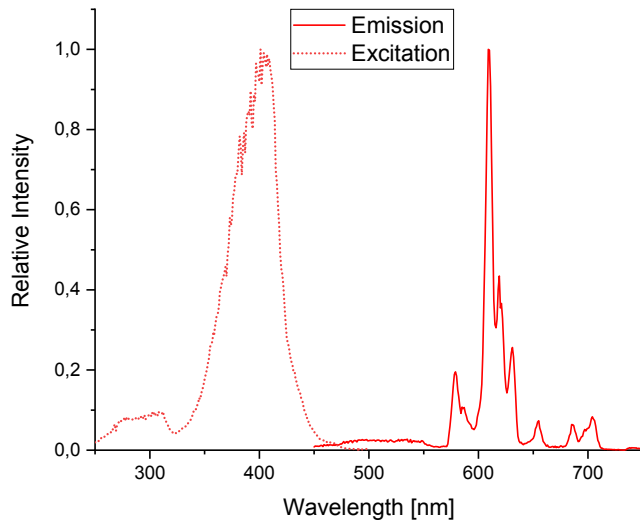


Fig. S18. Emission ($\lambda_{\text{ex}} = 360 \text{ nm}$) and excitation ($\lambda_{\text{em}} = 610 \text{ nm}$) spectra of Eu^{3+} complex **2** at 77 K in a $\text{CH}_2\text{Cl}_2/\text{MeOH}$ 1:1 glassy matrix.

Table S1. Lifetimes ($\lambda_{\text{ex}} = 376.7 \text{ nm}$), photoluminescence quantum yields ($\lambda_{\text{ex}} = 360 \text{ nm}$) and deactivation rate constants for Eu complex **2** at 77 K in a $\text{CH}_2\text{Cl}_2/\text{MeOH}$ 1:1 glassy matrix.

Emission wavelength (nm)	τ_1 ^{a)} (μs)	τ_2 ^{a)} (μs)	τ_{av} ^{b)} (μs)	Φ_L (%)	k_r (s ⁻¹)	k_{nr} (s ⁻¹)
580	908 ± 17 (10)	370 ± 4 (90)	430 ± 20	3 ± 2	80 ± 50	$(2.3 \pm 0.1) \times 10^3$
610	787 ± 14 (14)	372 ± 2 (86)	402 ± 6		80 ± 50	$(2.41 \pm 0.09) \times 10^3$
630	860 ± 30 (9)	383 ± 6 (91)	427 ± 9		80 ± 50	$(2.3 \pm 0.1) \times 10^3$

a) Relative amplitudes are given in parentheses as %. b) Amplitude-weighted average lifetime.

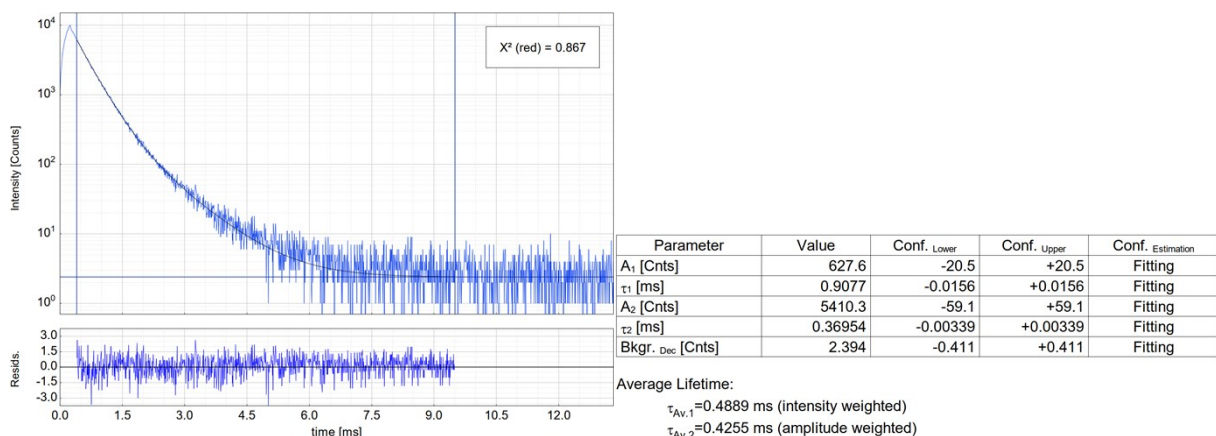


Fig. S19. Left: Time-resolved luminescence decay of Eu³⁺ complex **2** in a glassy matrix of CH₂Cl₂/MeOH 1:1 at 77 K, including the residuals ($\lambda_{\text{ex}} = 376.7$ nm, $\lambda_{\text{em}} = 580$ nm). Right: Fitting parameters including pre-exponential factors and confidence limits.

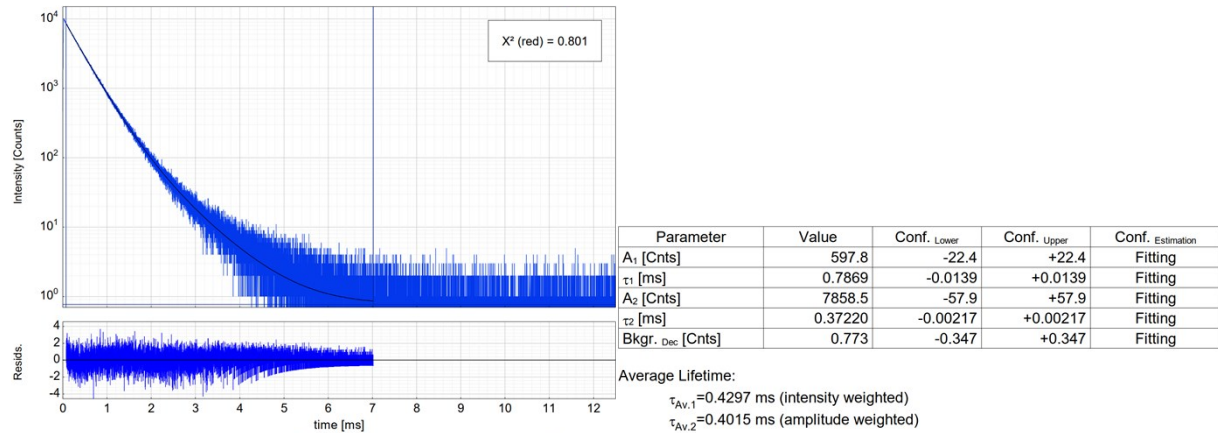


Fig. S20. Left: Time-resolved luminescence decay of Eu³⁺ complex **2** in a glassy matrix of CH₂Cl₂/MeOH 1:1 at 77 K, including the residuals ($\lambda_{\text{ex}} = 376.7$ nm, $\lambda_{\text{em}} = 610$ nm). Right: Fitting parameters including pre-exponential factors and confidence limits.

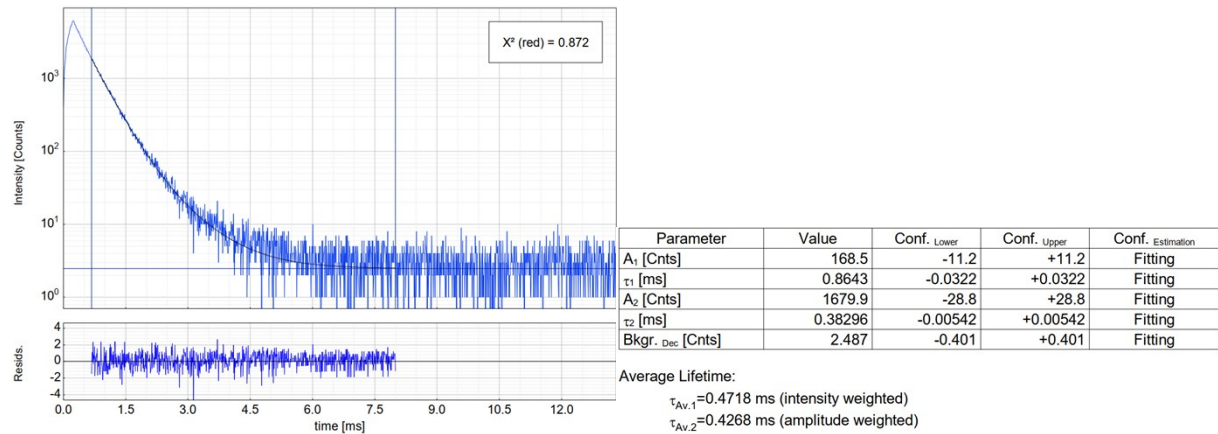


Fig. S21. Left: Time-resolved luminescence decay of Eu³⁺ complex **2** in a glassy matrix of CH₂Cl₂/MeOH 1:1 at 77 K, including the residuals ($\lambda_{\text{ex}} = 376.7$ nm, $\lambda_{\text{em}} = 630$ nm). Right: Fitting parameters including pre-exponential factors and confidence limits.

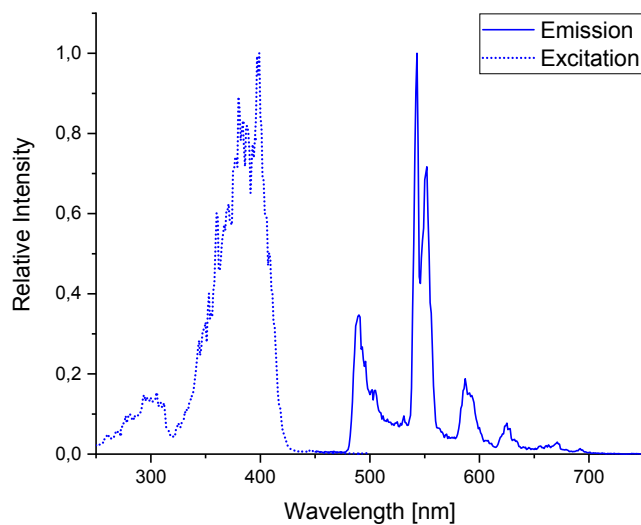


Fig. S22. Emission ($\lambda_{\text{ex}} = 360 \text{ nm}$) and excitation ($\lambda_{\text{em}} = 543 \text{ nm}$) spectra of Tb^{3+} complex **3** at 77 K in a $\text{CH}_2\text{Cl}_2/\text{MeOH}$ 1:1 glassy matrix.

Table S2. Lifetimes ($\lambda_{\text{ex}} = 376.7 \text{ nm}$), photoluminescence quantum yields ($\lambda_{\text{ex}} = 360 \text{ nm}$) and deactivation rate constants for Tb^{3+} complex **3** at 77 K in a $\text{CH}_2\text{Cl}_2/\text{MeOH}$ 1:1 glassy matrix

Emission wavelength (nm)	τ_1^{a} (μs)	τ_2^{a} (μs)	$\tau_{\text{av}}^{\text{b}}$ (μs)	Φ_L (%)	k_r (s ⁻¹)	k_{nr} (s ⁻¹)
490	1582 ± 15 (71)	565 ± 18 (29)	1040 ± 30	19 ± 2	180 ± 30	$(7.8 \pm 0.5) \times 10^2$
543	1484 ± 9 (71)	451 ± 8 (29)	900 ± 30		280 ± 40	$(1.19 \pm 0.07) \times 10^3$

a) Relative amplitudes are given in parentheses as %. b) Amplitude-weighted average lifetime.

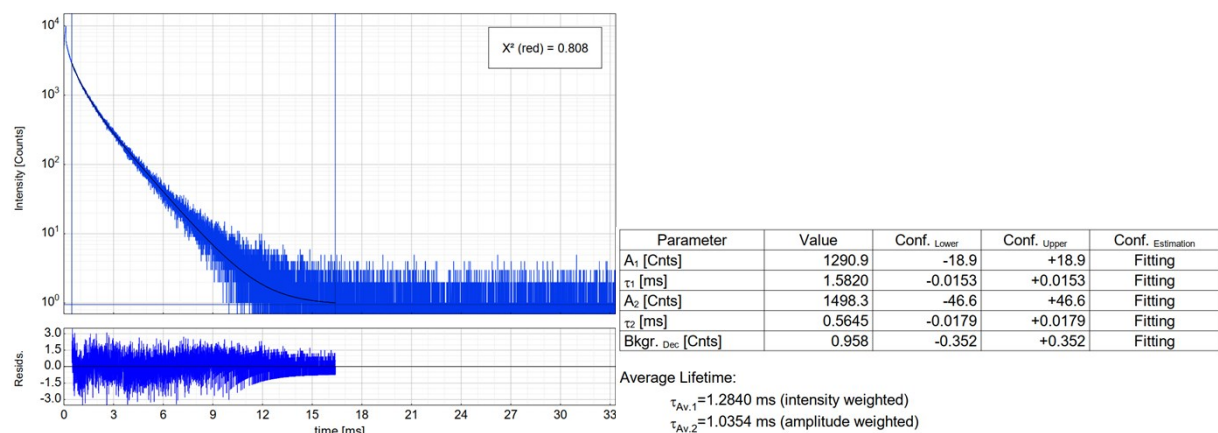


Fig. S23. Left: Time-resolved luminescence decay of Tb^{3+} complex **3** in a glassy matrix of $\text{CH}_2\text{Cl}_2/\text{MeOH}$ 1:1 at 77 K, including the residuals ($\lambda_{\text{ex}} = 376.7 \text{ nm}$, $\lambda_{\text{em}} = 490 \text{ nm}$). Right: Fitting parameters including pre-exponential factors and confidence limits.

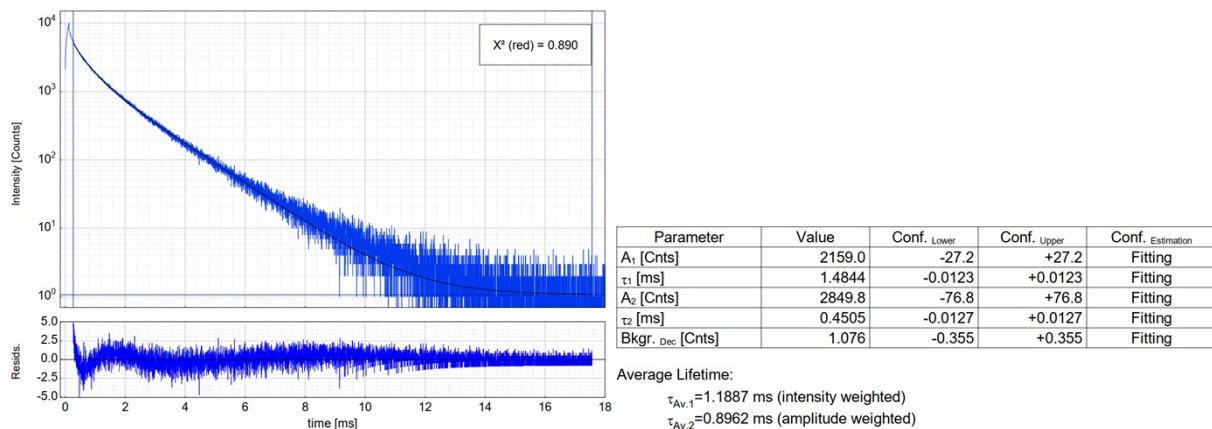


Fig. S24. Left: Time-resolved luminescence decay of Tb^{3+} complex **3** in a glassy matrix of $\text{CH}_2\text{Cl}_2/\text{MeOH}$ 1:1 at 77 K, including the residuals ($\lambda_{\text{ex}} = 376.7$ nm, $\lambda_{\text{em}} = 543$ nm). Right: Fitting parameters including pre-exponential factors and confidence limits.

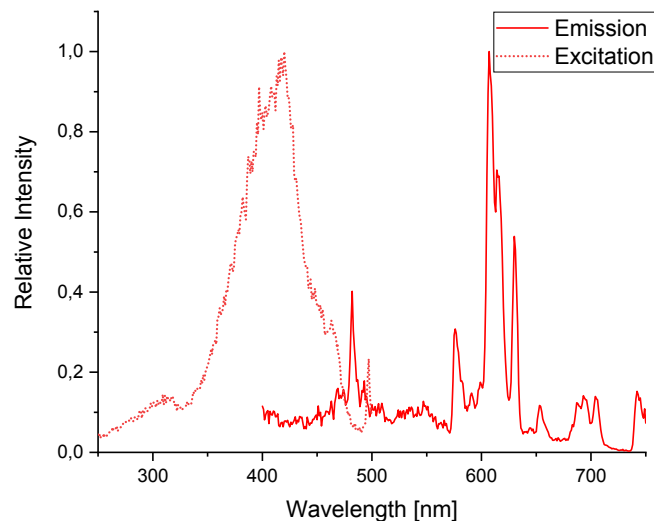


Fig. S25. Emission ($\lambda_{\text{ex}} = 360$ nm) and excitation ($\lambda_{\text{em}} = 607$ nm) spectra of Eu^{3+} complex **2** at 77 K in the solid state.

Table S3. Lifetimes ($\lambda_{\text{ex}} = 376.7$ nm), photoluminescence quantum yields ($\lambda_{\text{exc}} = 360$ nm) and deactivation rate constants for Eu^{3+} complex **2** at 77 K in the solid state.

Emission wavelength (nm)	τ_1 ^a (μs)	τ_2 ^a (μs)	τ_{av} ^b (μs)	Φ_L (%)	k_r ^c (s ⁻¹)	k_{nr} ^d (s ⁻¹)
607	258 ± 3 (31)	90 ± 1 (69)	143 ± 4	< 2	< 140	$(6.98 > k_{\text{nr}} > 6.84) \times 10^3$
630	253 ± 3 (31)	87 ± 2 (69)	139 ± 4		< 144	$(7.20 > k_{\text{nr}} > 7.06) \times 10^3$

^a) Relative amplitudes are given in parentheses as %. ^b) Amplitude-weighted average lifetime. ^c) The upper limit of the Φ_L is used for the calculation. ^d) The upper and lower limits of the Φ_L are used to calculate k_{nr} .

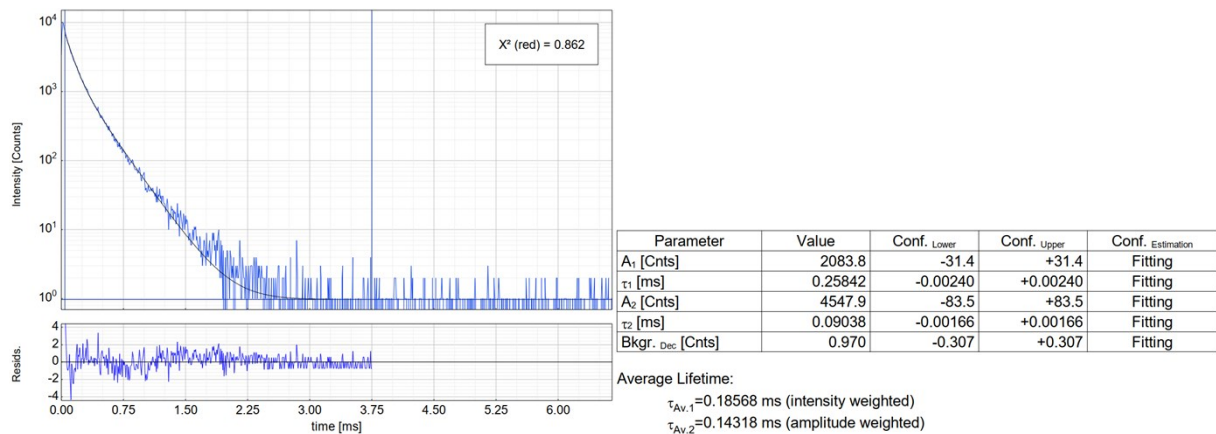


Fig. S26. Left: Time-resolved luminescence decay of Eu^{3+} complex **2** in the solid state at 77 K, including the residuals ($\lambda_{\text{ex}} = 376.7$ nm, $\lambda_{\text{em}} = 607$ nm). Right: Fitting parameters including pre-exponential factors and confidence limits.

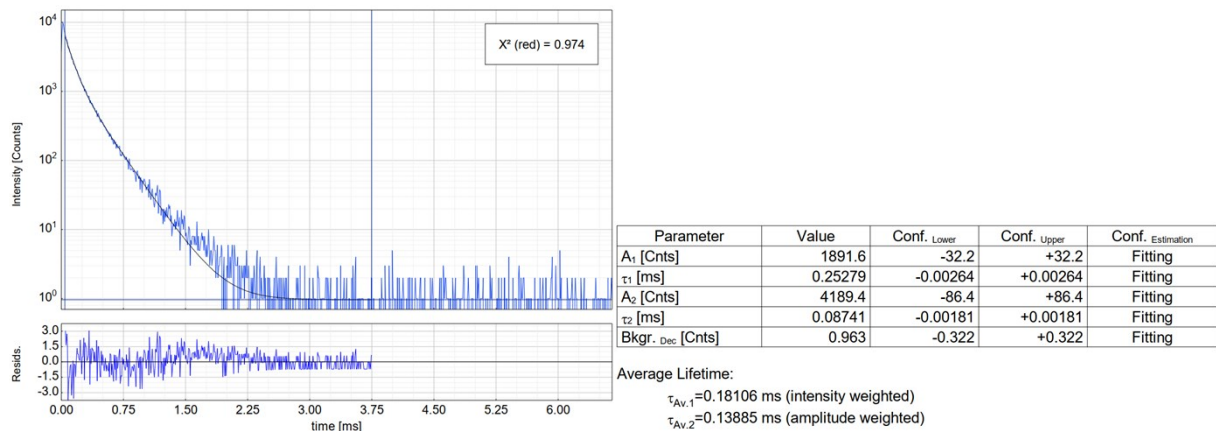


Fig. S27. Left: Time-resolved luminescence decay of Eu^{3+} complex **2** in the solid state at 77 K, including the residuals ($\lambda_{\text{exc}} = 376.7$ nm, $\lambda_{\text{em}} = 630$ nm). Right: Fitting parameters including pre-exponential factors and confidence limits.

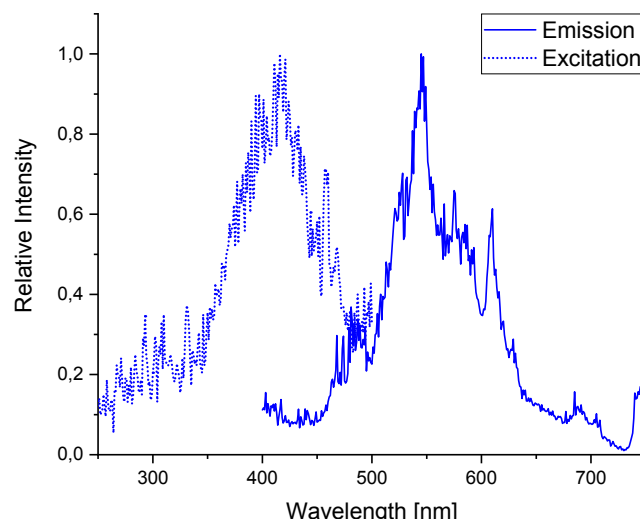


Fig. S28. Emission ($\lambda_{\text{ex}} = 360$ nm) and excitation ($\lambda_{\text{em}} = 550$ nm) spectra of Tb^{3+} complex **3** at 77 K in the solid state.

Table S4. Lifetimes ($\lambda_{\text{ex}} = 376.7$ nm), photoluminescence quantum yields and deactivation rate constants of Tb^{3+} complex **3** at 77 K in the solid state ($\lambda_{\text{ex}} = 360$ nm)

Emission wavelength (nm)	τ_1^{a}	τ_2^{a}	$\tau_{\text{av}}^{\text{b)}$	Φ_L^{c} (%)	k_r^{c} (s ⁻¹)	k_{nr}^{d} (s ⁻¹)
500	2.6 ± 0.1 ns (22)	0.41 ± 0.01 ns (78)	0.50 ± 0.03 ns	< 2	< 4×10^7	($1.26 > k_{\text{nr}} > 1.23$ x 10 ⁹)
550	62 ± 1 μ s (27)	17.7 ± 0.06 μ s (73)	29 ± 1 μ s		< 6.9×10^2	($3.49 > k_{\text{nr}} > 3.42$ x 10 ⁴)

^{a)} Relative amplitudes are given in parentheses as %. ^{b)} Amplitude-weighted average lifetime. ^{c)} The upper limit of the Φ_L is used for the calculation. ^{d)} The upper and lower limits of the Φ_L are used to calculate k_{nr} .

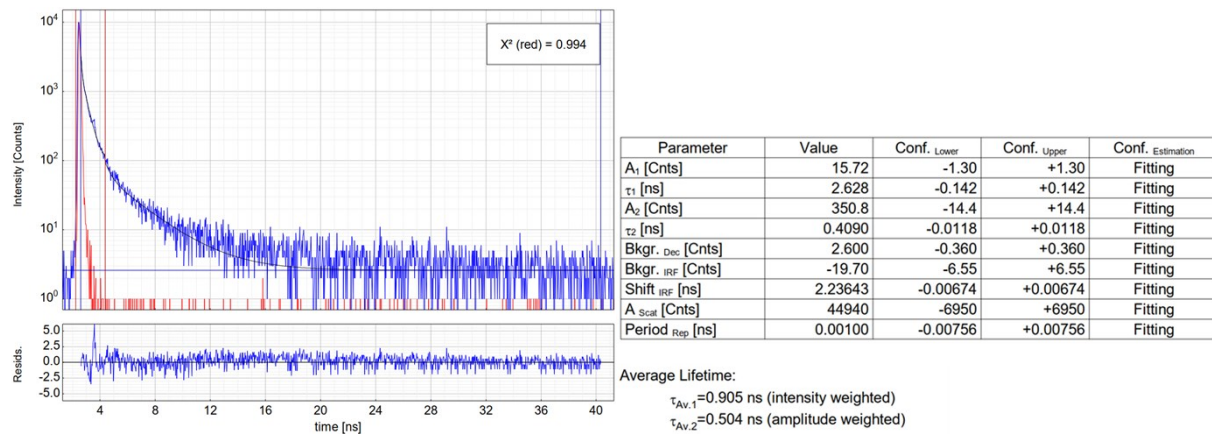


Fig. S29. Left: Time-resolved luminescence decay of Tb^{3+} complex **3** in the solid state at 77 K ($\lambda_{\text{ex}} = 376.7$ nm, $\lambda_{\text{em}} = 500$ nm). Right: Fitting parameters including pre-exponential factors and confidence limits.

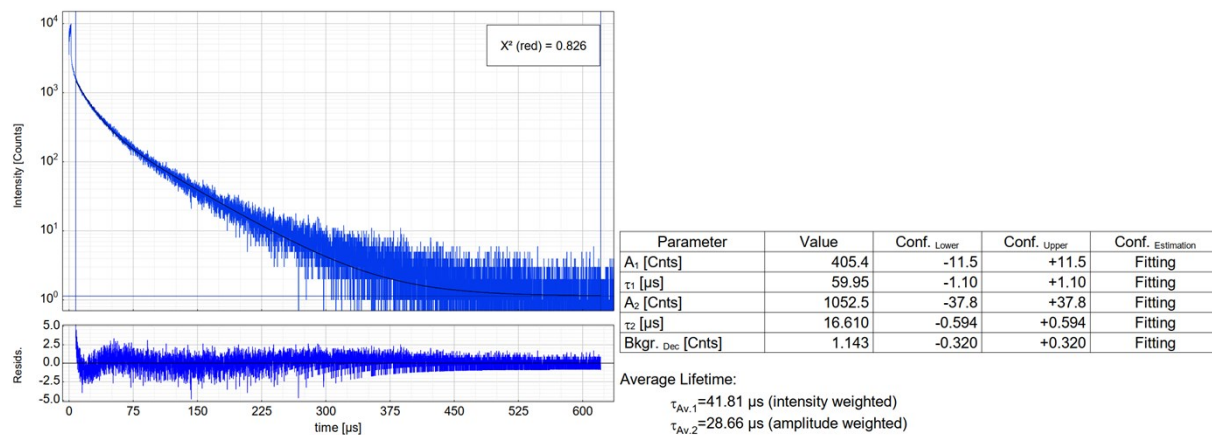


Fig. S30. Left: Time-resolved luminescence decay of Tb^{3+} complex **3** in the solid state at 77 K, including the residuals ($\lambda_{\text{ex}} = 376.7$ nm, $\lambda_{\text{em}} = 550$ nm). Right: Fitting parameters including pre-exponential factors and confidence limits.

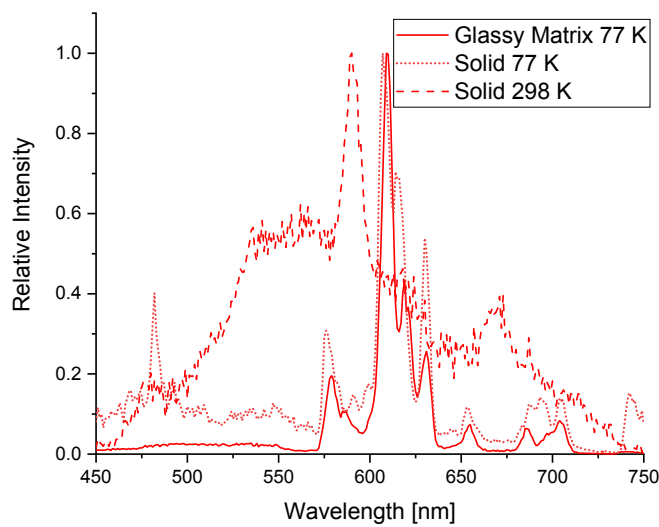


Fig. S31. Emission spectra ($\lambda_{\text{ex}} = 360 \text{ nm}$) of Eu³⁺ complex **2** at 77 K in a CH₂Cl₂/MeOH 1:1 glassy matrix and solid state and at 298 K as a powder.

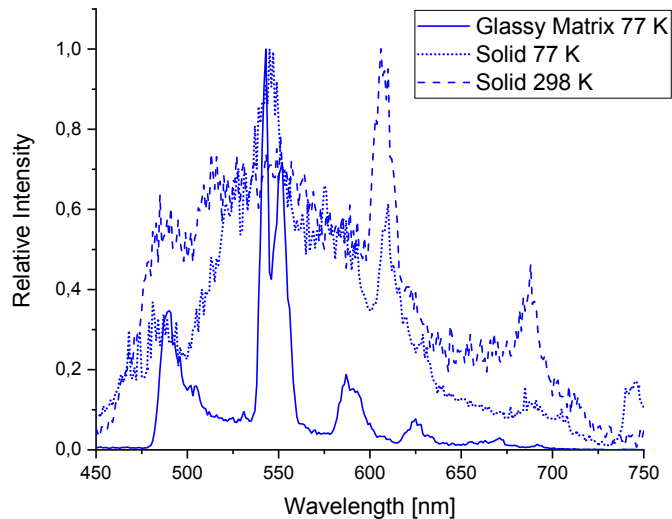


Fig. S32. Emission spectra ($\lambda_{\text{ex}} = 360 \text{ nm}$) of Tb³⁺ complex **3** at 77 K in a CH₂Cl₂/MeOH 1:1 glassy matrix and in the solid state and at 298 K as a powder.